Solvent Extraction and Ion Exchange, 25: 857–877, 2007

ISSN 0736-6299 print/1532-2262 online
DOI: 10.1080/07366290701634610

Separation of Zinc by a Non-dispersion Solvent Extraction Process in a Hollow Fiber Contactor

E. A. Fouad
High Institute of Technology, Benha University, Benha, Egypt

H.-J. Bart
TU Kaiserslautern, Thermische Verfahrenstechnik, Kaiserslautern, Germany

Abstract: A process for recovery of zinc from acid solution with di(2-ethyl hexyl phosphoric acid) (D2EHPA) dissolved in iso-dodecane was carried out at 20°C in a countercurrent tubular membrane extractor using a hollow fiber as solid support. Experiments were performed at different aqueous metal concentrations (0.1–1.0 g/L), pH 0.1–2.1, and D2EHPA concentrations (2–8 v%). It was found that both the flux of metal and the extraction extent was highly influenced by the extractant concentration and the pH of the feed solution. Overall mass transfer coefficients were determined and related to the tube side, the membrane, and the shell side mass transfer by varying the aqueous flow rate (0.38–0.80 L/min) and organic flow rate (0.22–0.57 L/min) in countercurrent flow. The overall mass transfer coefficient for zinc extraction ranged from 6.2×10^{-6} m/s to 25.3×10^{-6} m/s. It was concluded that extraction kinetics were a major contributor to the overall resistance to mass transfer.

Keywords: Zinc, D2EHPA, hollow fiber membrane, non- dispersive solvent extraction

INTRODUCTION

Conventional solvent extraction has been used in the chemical industry for over a century. The main challenge in designing and operating a solvent

Received 24 May 2007, Accepted 25 July 2007
Address correspondence to E. A. Fouad, High Institute of Technology, Benha University, Benha, Egypt. E-mail: sayedfou@yahoo.com

extraction operation is the maximization of the mass transfer by producing as much interfacial area as possible between the stripped feed and the solvent which is generally immiscible with the stripped feed. This is achieved by dispersion in mixer-settlers devices or by a judicious selection of the packing material in columns. However, this conventional equipment has many disadvantages: the need of dispersion and coalescence, problems of emulsification, flooding and loading limits in continuous countercurrent devices, the need for an appropriate density difference between the phases, and the high maintenance costs of centrifugal apparatus.[1]

Independently of the achievements in extraction chemistry, in recent years attention has been also paid to develop new high-efficiency equipment for solvent extraction.[2,3] A liquid membrane is a liquid phase that separates two other liquid phases with which it is immiscible.[4] During the past years, the use of liquid membranes has gained a general interest in the separation and concentration of metallic species in hydrometallurgical processes and may also be used in wastewater treatment where solute concentrations are low and large volumes of solutions must be processed.[5–7]

One of the promising ideas is the use of microporous hollow fiber modules (HFMs) as liquid/liquid phase contactors.[8] HFMs represent a very attractive solution to the need of operating membrane modules allowing very high throughputs. With HFMs modules, membrane-packaging densities as high as $1000\ m^2/m^3$ can be reached. This value compares to about $500\ m^2/m^3$ for the plate and the frame and to about $50\ m^2/m^3$ for tubular membrane modules. Moreover, HFMs modules are characterized by low investment and operating costs because of the reduced hardware and the favorable hydrodynamics that minimizes aqueous concentration polarization effects and membrane fouling.[9]

The basic principle of non-dispersive extraction is the immobilization of the interface in the pores of hydrophobic membranes, due to wetting and appropriate applied static pressure.[8,10] The main advantages of this method are the following: no entrainment; no flooding; very large interfacial area; the possibility to realize extreme phase ratios; independency of phase densities, and interfacial tension.[11] A shortcoming of HFM extraction could be blinding with particles in the feed (prefiltration might be necessary). Recently, great attention for the extraction of heavy metal ions with hollow fiber modules made of different material fibers were studied for improving the performance of the mass transfer and describing the extraction mechanism.[12–26]

Heavy-metal-contaminated wastewaters usually contain a mixture of different cations and anions. For example, Cu, Zn, Ni, etc., are present as cations, whereas Cr(VI), Hg, Cd, etc., are commonly found as anions. To prevent pollution and achieve resource recovery/recycling, heavy metals are to be recovered individually from such waste streams and concentrated. Selective solvent extraction/concentration of individual heavy metals is an attractive option.

The concept of our contribution concerns the feasibility of HFM for zinc extraction from sulfate medium by D2EHPA extractant diluted in isododecane, with the aim to characterize possible and optimal operation conditions regarding the throughputs of the phases and the possible enrichment in the extraction circle. To evaluate the performance of HFMs as extraction devices, two different initial zinc concentrations were chosen, both representing different applications. The so-called "100 ppm concept" (initial zinc concentration equals 100 mg/L) stands for environmental engineering; the "1000 ppm concept" (initial zinc concentration equals 1000 mg/L) represents hydrometallurgical applications. In both cases the main criteria were, according to their importance, high depletion of the metal ion concentration in the raffinate (at least 2 orders of magnitude), maximum possible volumetric flow rate of the aqueous raffinate phase, and enrichment of metals (into the stripping phase) via an extraction/reextraction cycle (by variation of phase ratio and/or concentration of complexing agent). The overall mass transfer coefficient is calculated and plotted versus time from the data obtained experimentally in the extraction process. The percentage extraction of zinc at feed pH of 0.1 and 2.1 are presented.

EXPERIMENTAL

Hollow-Fiber Contactor

The experiments were carried out on a microporous hollow fiber membrane module produced by Celgard (Celgard GmbH, Germany). This geometry allows a very large contact area with a minimal volume high compactness. As the membrane material was hydrophobic, the pores were filled with the organic solution. The module displayed a cross-flow configuration. This was ensured by a baffle located in the middle of the fiber bundle (see Fig. 1), which compelled the aqueous solution to flow from the porous distribution tube located in the center of the fiber bundle to the wall of the shell in the first chamber and vice-versa to the collection tube in the second chamber. This was meant to promote turbulence in the fluid flowing outside the fibers, therefore, improving the mass transport through the boundary layer around the fibers. The geometric characteristics of the module are detailed in Table 1.

Chemicals and Materials

The source for zinc was $ZnSO_4 \cdot 7H_2O$, of analytical grade (Fisher Scientific). The pH was adjusted to the desired value by continuous drop addition of 1% (v/v) sulfuric acid or 5 N NaOH prepared with analytical grade reagents. The cation exchanger D2EHPA from Baysolvex BAYER with 0.5% monoacid and

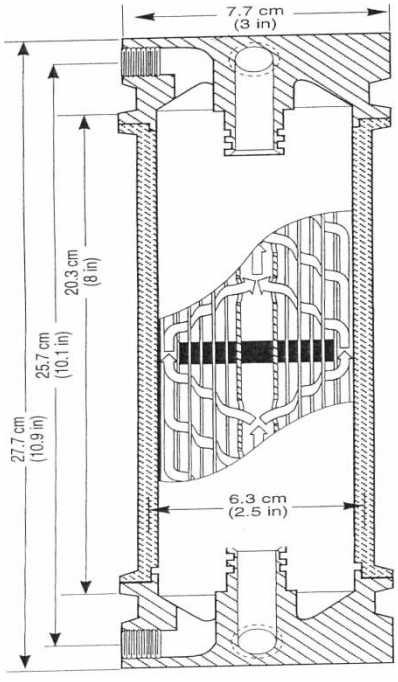

Figure 1. Liquicel extra-flow hollow fiber contactor.

2.2% mass neutral impurities mainly 2-ethylhexanol was used without purification. Gefachem–Prochemie, Leverkusen, supplied the high purity isododecane, used as a solvent for D2EHPA. All the other reagents were standard chemicals of analytical grade and were used without any further purification. The extraction system was investigated between 0.1 g/L and 1.0 g/L Zn^{2+}, which is typical for metal extraction in hydrometallurgy, with 2v% to 8v% D2EHPA and a pH-range from 0.1 to 2.1. The aqueous samples were analyzed for metal content using a Hitachi Z8100 atomic absorption spectrophotometer. A mass balance provided the organic phase concentration.

Hollow-fiber Experiments

The hollow fiber membrane unit is completely automatically controlled by Lab Vision control software. Pumping of the feed and organic phases was achieved by using MCP-Z pumps capable of flows up to 1250 mL/min. Teflon flow meters, situated at the inlet of the HF module, were used to monitor the flow rates of the feed, and organic phases. Pressure gauges are panel-mounted to measure the inlet/outlet pressures and flows for both the tube side and the shell side (see Fig. 2). Separation experiments were carried out at room temperature (20°C).

Table 1. Geometric characteristics of the tested hollow fiber contactor

Provider: Contactor type	Hoechst Celanese Corporation Celgard X-30 Microporous Polypropylene Hollow Fiber [Liqui-Cel extra-flow 2.5 in. × 8 in. (64 mm × 203 mm)]
Shell diameter	6.3 cm
Fiber bundle diameter	4.7 cm
Distribution tube diameter	2.2 cm
Effective surface area	1.4 m^2
Effective fiber length	15 cm
Effective Area/Volume	29.3 cm^2/cm^3
Number of fibers	9950
Outer fiber diameter	300 μm
Inner fiber diameter	240 μm
Fiber wall thickness	30 μm
Fiber porosity	0.4
Pore tortuosity	2.25
Effective pore diameter	0.03 μm

In all the experiments involving the HFM, we chose to run the aqueous feed in the lumen side and the organic in the shell side because the membrane is hydrophobic, as can be seen in Fig. 1b. Since the organic solvent wets the membrane spontaneously, we applied a positive static pressure to the aqueous phase to prevent the organic from dispersing into the aqueous feed to form an emulsion. If we ran the organic in the lumen, it would be harder to apply such a pressure from the shell side.[27]

The aqueous phase flowed countercurrently to the organic extractant and the pressure in the aqueous phase was held 0.2–0.5 bar higher than the pressure in the organic phase. This pressure difference allowed a stable aqueous/organic interface to be maintained at the shell side of the membrane. Both the aqueous and organic phases were recycled totally (100%). The aqueous and organic initial volumes were 4L and 1L respectively, and the samples were approximately 3 mL. Samples were taken at 1, 2, 3, 5, 7, 10, 20, 30, 40, 60, 80, 100, 120, 150, 180, 240, and 300 minutes to follow the extraction.

Theory

Solvent Extraction of Zinc

The extraction of zinc from an aqueous to a solvent phase containing D2EHPA is characterized by the extraction reaction presented in Eq. (1):

$$Zn^{2+} + n(HR)_2 \rightleftharpoons ZnR_2(HR)_{2(n-1)} + 2H^+ \quad (1)$$

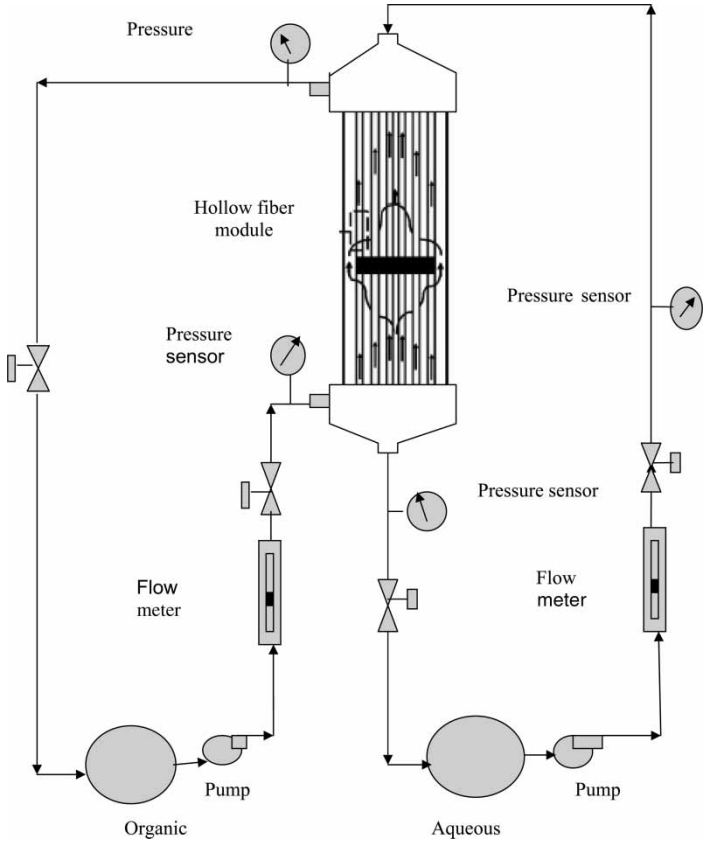

Figure 2. Experimental setup. The aqueous feed flows in the lumen, and the organic is in the shell side.

The distribution coefficient m is dependent on the pseudo-equilibrium constant for the reaction, K_{ext}, the pH of the aqueous solution and the solvent extractant concentration, as shown in Eq. (2). At low solvent loading $n = 1.5$[28] and K_{ext} is constant for a given temperature and ionic strength:

$$K_{ext} = \frac{[ZnR_2(HR)_{2(n-1)}] \cdot [H^+]^2}{[Zn^{2+}] \cdot [(HR)_2]^n} = m \cdot \frac{[H^+]^2}{[(HR)_2]^n} \tag{2}$$

Mass Transfer in a Hollow Fiber Contactor

The overall apparent mass transfer coefficient can be defined by considering an overall mass balance (aqueous phase):

$$-Q_w dC_w = k_w(C_w - C_w^*)dA \tag{3}$$

Where C_w^* is the solute concentration at the aqueous-organic interface. The experimental conditions used for this study were chosen to minimize resistance in the membrane and solvent phases. Under these conditions $C_w^* << C_w$, leading to the simplification that $C_w - C_w^* \cong C_w$. Integrating over the module leads to Eq. (4) which enables the calculation of experimental overall mass transfer coefficients for aqueous flowing in either the shell or the tube side of the module.

$$k_w = \frac{Q_w}{A} \ln\left(\frac{C_w^{in}}{C_w^{out}}\right) \tag{4}$$

Mass transfer in a hollow fiber contactor can be described using a conventional resistance-in-series model.[29] When mass transfer is transport limited, the overall mass transfer coefficient (k_w), for extraction of a solute from an aqueous to a solvent phase (based on aqueous in the tube side), can be represented by Eq. (5).[30] The underlying assumption, when applying this model to describing zinc mass transfer, is that the chemical reaction described by Eq. (1) is fast and reaches equilibrium at the interface:

$$\frac{1}{k_w} = \frac{1}{k_t} + \frac{d_i}{mk_m d_{lm}} + \frac{d_i}{mk_s d_o} \tag{5}$$

Where: $d_{lm} = d_o - d_i/\ln(d_o/di)$

The local mass transfer coefficients for the boundary layer resistance in the tube side, diffusion of the solute in the membrane pores, and the boundary layer resistance in the shell side, are given by k_t, k_m, and k_s, respectively. With the aqueous phase in the shell side, the aqueous–organic interface is on the outside surface of the lumen and Eq. (6) can be:

$$\frac{1}{K_w} = \frac{d_o}{mk_i d_i} + \frac{d_o}{mk_m d_{lm}} + \frac{1}{k_s} \tag{6}$$

For laminar flow in the tube side of the membrane, the tube side local mass transfer coefficient is related to the Sherwood number using the Leveque approximation,[31] according to Eq. (7):

$$Sh_t = \frac{k_t d_i}{D_w} = 1.62 Sc^{1/3}\ Re^{1/3}\left(\frac{d_i}{L}\right)^{1/3} \tag{7}$$

In the membrane, the local mass transfer coefficient can be calculated from known membrane parameters of solute diffusivity (D_{org}), membrane thickness (δ), tortuosity (τ) and porosity (ε), according to Eq. (8).[29] The diffusivity is for the organic phase, D_{org}, because the membrane is hydrophobic and is wetted by the organic.

$$k_m = \frac{D_{org}\varepsilon}{\delta\tau} \tag{8}$$

Mass transfer correlations on the shell side depend on the type of flow within the module. For cross-flow hollow fiber modules, a significant portion of the flow is

perpendicular to the lumen bundle and various approaches have been used. The conventional approach is to define the Sherwood number in terms of the outer fiber diameter, d_o, as shown in Eq. (9). The Reynolds number is also defined with d_o as the characteristic length. The superficial velocity is calculated as the flow rate through the shell divided by the cross-sectional area. Where flow in a cross-flow module is radial, the cross-sectional area varies with diameter and the arithmetic average area is used.[32] The effective velocity is then calculated as the superficial velocity divided by the void fraction.

$$Sh_s = \frac{k_s d_o}{D_s} = \alpha Sc_s^{1/3} Re_s^{\beta} \tag{9}$$

Where α and β are the shell side correlation coefficients. Schoner et al.[33] developed a modified approach to shell side correlations in cross-flow modules where the characteristic length and velocity calculations were adapted specifically for cylindrical cross-flow modules. In this case, in the calculation of the Sherwood number, the hydraulic diameter, d_h, replaced d_o, which was calculated, as per Eq. (10), and the superficial velocity was defined as the log mean average velocity, as shown in Eq. (11):

$$d_h = \frac{4 \text{ volume of voids filled with fluid}}{\text{wetted surface area of the bed}} = \frac{4V_m}{A} = \frac{d_{so}^2 - d_{si}^2 - nd_{hf}^2}{nd_{hf}} \tag{10}$$

$$\upsilon_s = \frac{Q_s}{\pi(L/2)} \cdot \frac{\ln(d_{so}/d_{si})}{(d_{so} - d_{si})} \tag{11}$$

RESULTS AND DISCUSSION

Different variables were studied to investigate their influence on Zn^{2+} extraction by D2EHPA using NDSX technique. Overall mass transfer coefficient (k_w) is calculated according to Eq. (4). According to the literature,[34] zinc extraction may be controlled by various steps:

1. diffusion of metal ions in the aqueous phase;
2. diffusion of the hydrogen ions in the aqueous phase;
3. diffusion of metal complex through the organic membrane phase;
4. diffusion of the complexing agent through the organic membrane phase;
5. diffusion of the metal complex in the bulk organic phase;
6. diffusion of the complexing agent in the bulk of organic phase.

1. Effect of carrier concentration

To study the effect of the extractant concentration, experiments were done with different D2EHPA concentrations in iso-dodecane at pH 2.01. The

variation of the overall mass transfer coefficient (k_w) with time at different D2EHPA concentrations is shown in Fig. 3. From these data, it is observed that the increase of D2EHPA concentration accounts for a drastic increase of the overall mass transfer coefficient. Furthermore, it is found that, the interfacial reaction resistance has a great affect on the extraction of zinc in hollow fiber contactors and may not be neglected.[35]

2. Effect of zinc concentration in aqueous phase

The effect of feed concentration on the extraction of zinc is shown in Fig. 4. The percentage extraction varied with the change in feed concentration. We found that the overall mass transfer coefficient, which was largely independent of feed concentration, depends on initial feed concentrations as shown in Fig. 4. This observation is similar to the result observed by Yang and Cussler[27] for the extraction of copper and nickel. This increase suggests that the

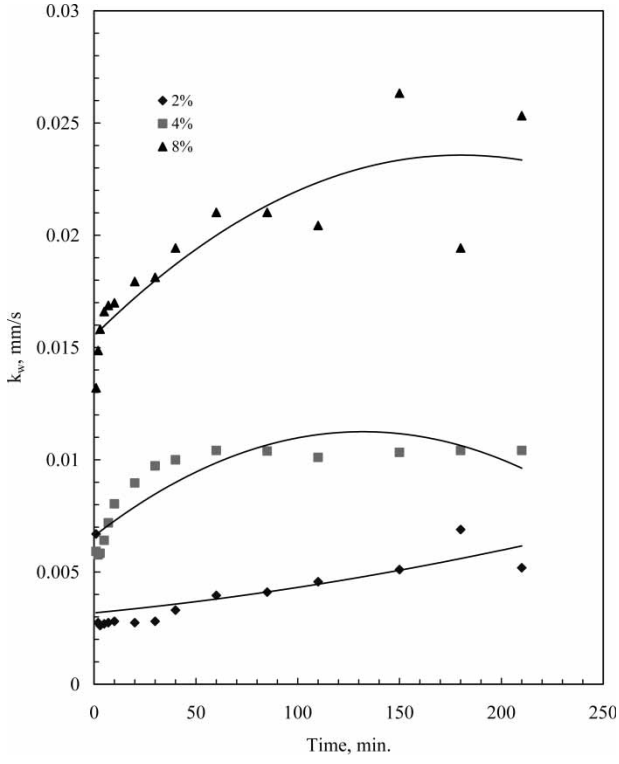

Figure 3. Effect of D2EHPA concentration on the overall mass transfer coefficient of Zn.

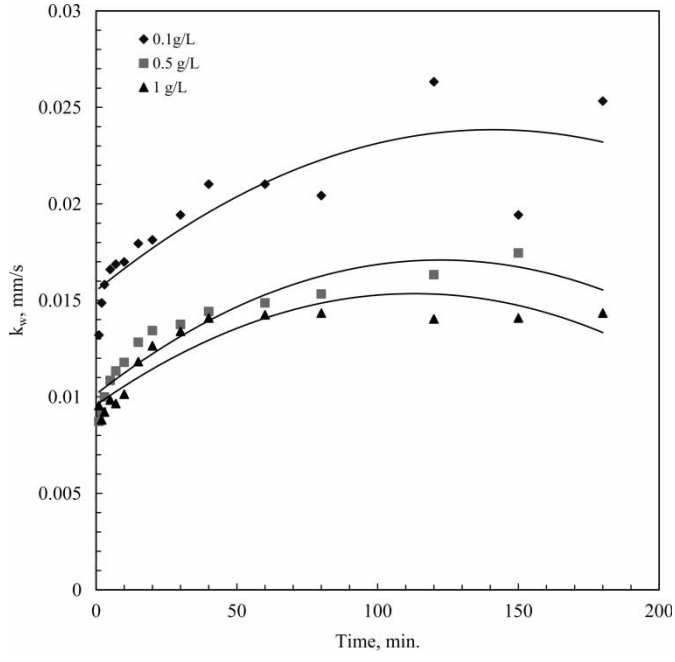

Figure 4. Variation of overall mass transfer coefficient with time at different feed concentration.

carrier molecules were unsaturated at smaller feed concentration and they could be used for extracting higher concentrated feeds.

3. Effect of aqueous phase acidity

The values of k_w are calculated at feed pH 0.1 and pH 2.01 and are plotted in Fig. 5. The k_w values varied with pH. This could be the effect of less extraction at lower pH where the concentration of the zinc is smaller. This reflects the use of D2EHPA, which is an acidic extractant.

4. Effect of aqueous flow rate (Q_w) on the overall mass transfer coefficient

The outlet concentrations of zinc in the aqueous phase, C_w^{out}, as a function of aqueous phase flow rate, Q_w, are shown in Fig. 6. By investigating Fig. 6, we can show that zinc concentration reaches 0.23 the initial concentration after 5 minutes. With increasing the cycle time up to 120 minutes,

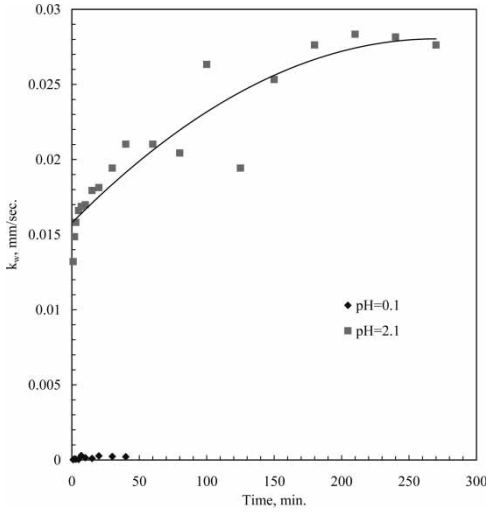

Figure 5. Variation of overall mass transfer coefficient with time at different feed acidity.

the zinc concentration reaches 0.12 of the initial feed concentration. These data show that a very high level of zinc removal was easily achieved at low aqueous flow rates. One can see the presence of high interfacial area in hollow fiber membrane contactor for the complexation of zinc with

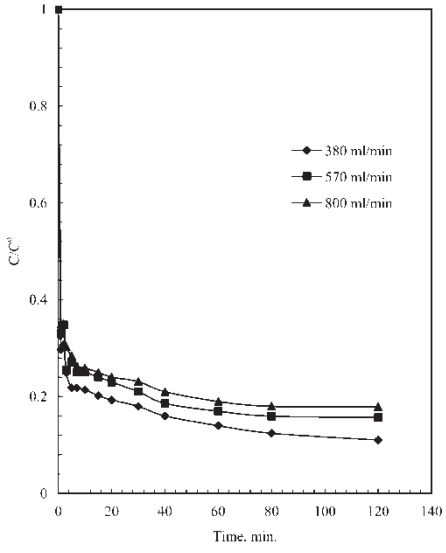

Figure 6. Effect of aqueous flow rate on Zn concentration in the outlet aqueous phase.

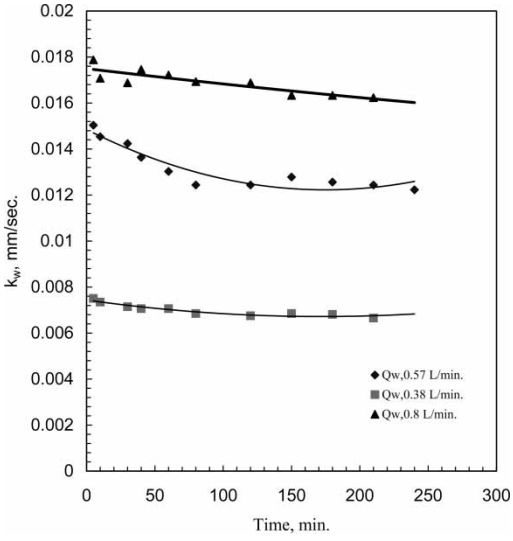

Figure 7. Variation of overall mass transfer coefficient with time at different aqueous flow rate.

D2EHPA. Figures 7 and 8 are a plot of the overall mass transfer coefficient, k_w, vs the aqueous flow rate, Q_w and time. It was observed from Fig. 7 that the mass transfer coefficient decreased slightly with time for the low aqueous flow rate, whereas this reduction was observed as the aqueous

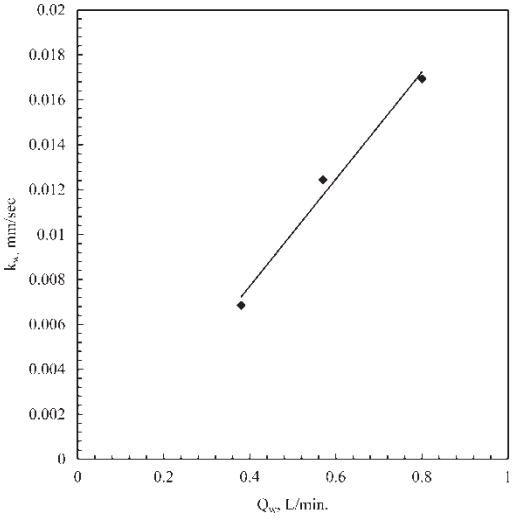

Figure 8. Effect of aqueous flow rate on Zn mass transfer coefficient based on aqueous phase.

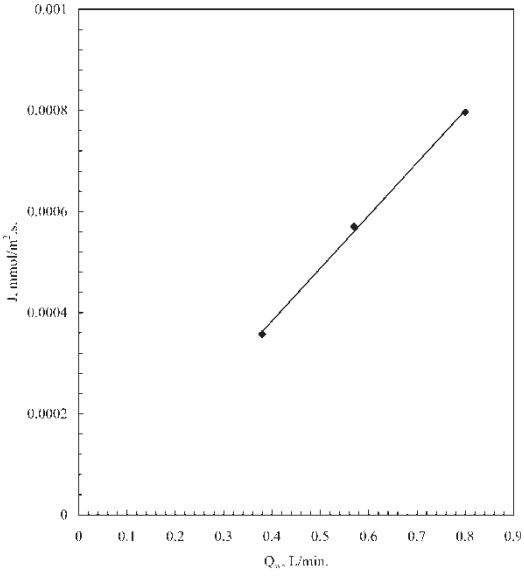

Figure 9. Variation of the mean Zn flux through the interfacial area with aqueous feed flow rate.

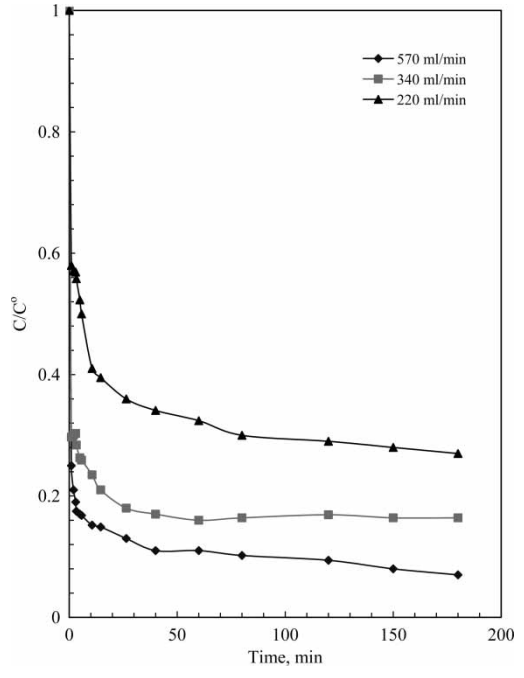

Figure 10. Effect of organic flow rate on Zn concentration in outlet aqueous phase.

flow rate increased from 0.38 l/min to 0.8 l/min. This reflects the increase in the zinc extraction with increasing the flow rate and then decreasing the aqueous feed concentration with time. This influences the concentration gradient through the aqueous boundary layer and hence the mass transfer coefficient decreased. A linear dependence was obtained (Fig. 8), indicating that the mass-transfer coefficient implying the aqueous boundary layer resistance is an important contributor to the total mass-transfer resistance. The same type of linear dependence was reported for the removal of heavy metals from wastewater and thallium.[14,35]

The mean flux J of Zn^{2+} through the interfacial area A is calculated according the following equation:[14]

$$J = \frac{1}{A}\int_0^A JdA = \frac{Q_w}{\pi d_i nL}\left(C_w^{in} - C_w^{out}\right) = k_w \Delta C_{lm} \tag{12}$$

In Fig. 9 the mean flux of zinc is plotted against the aqueous phase flow rate. The zinc flux through the interfacial area increases with increasing aqueous phase flow rate due to an increase in both ΔC_{lm} and k_w. Similar relations

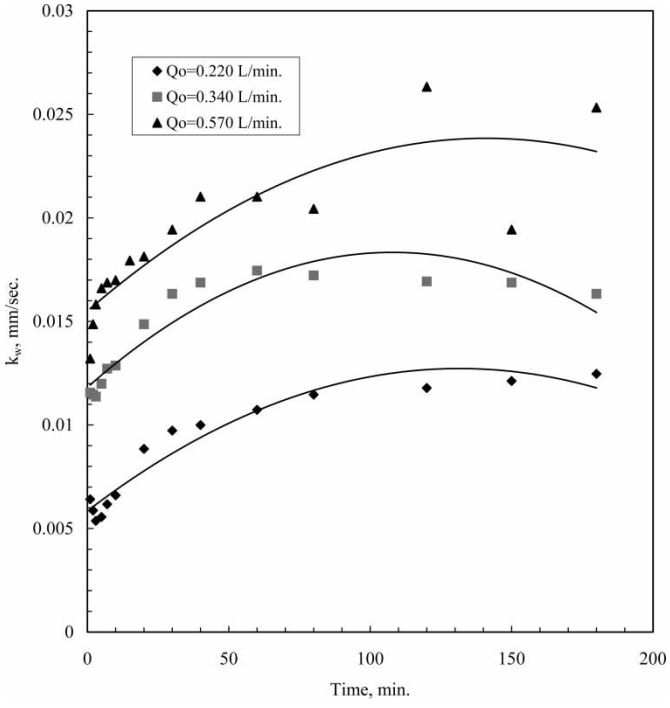

Figure 11. Variation of overall mass transfer coefficient with time at different organic phase flow rate.

between J and Q_w are also reported elsewhere.[8,14,36] At sufficiently high phase flow rates; the membrane resistance and the inlet zinc concentration in the feed stream limit the zinc flux.

5. Effect of the organic flow rate (Q_o) on the overall mass transfer coefficient

Figure 12 show the dependence of the overall mass transfer coefficient, k_w, on the organic phase flow rate, Q_o, at a constant feed flow rate of 800 ml/min. Thus, an increase in the flow rate of D2EHPA in iso-dodecane significantly increases the zinc extraction rate and reduces zinc concentration in the aqueous outlet solution (see Figs. 10, 11). This implies that the organic boundary layer resistance plays an important role in the zinc extraction rate.

From Figs. 3, 8, 9, and 12 it may be concluded that all three resistances, namely, the organic boundary layer resistance, the interfacial reaction resistance, and the aqueous boundary layer resistance affect the zinc extraction rate and the mass-transfer coefficient; further the organic boundary layer resistance plays a key role in the zinc extraction rate in the HFM extractor.

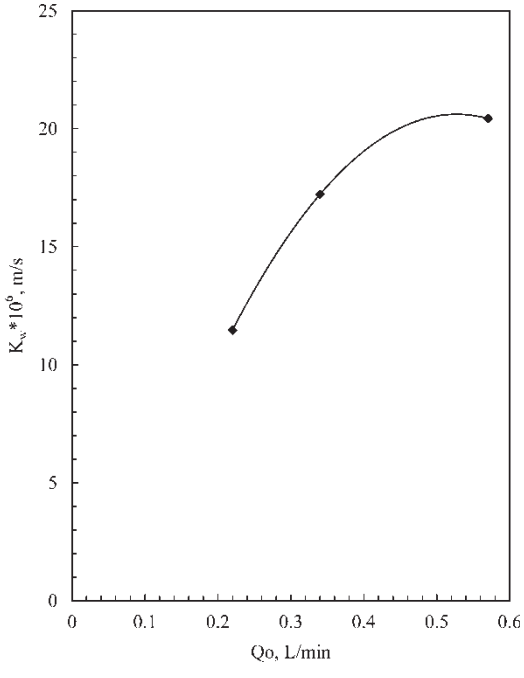

Figure 12. Variation of overall mass transfer coefficient with organic phase flow rate.

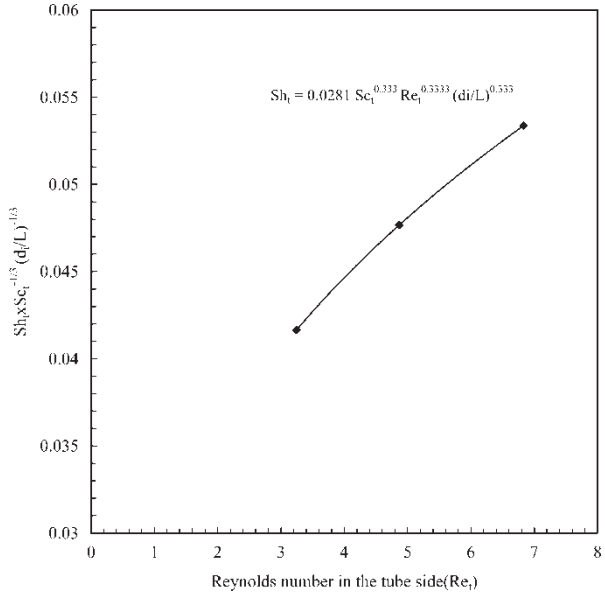

Figure 13. Mass transfer correlations in the tube side of Celgard Liqui-Cel extra-flow contactor.

6. Estimation of the mass transport correlations

For the tube side, the experimental data is correlated using Eq. (7), with Sh_t and Re_t defined according to the following equations:

$$Sh_t = \frac{k_t d_i}{D_{Zn}} \tag{13}$$

$$Re_t = \frac{4Q_w}{\eta_w n \pi d_i} \tag{14}$$

$$Sc_t = \frac{\eta_w}{D_{Zn}} \tag{15}$$

On the other side, Sh_s and Re_s for the shell side defined according to Equations (16) and (17):

$$Sh_s = \frac{k_s d_h}{D_{ZnA_2}} \tag{16}$$

$$Re_s = \frac{\upsilon_s \cdot d_h}{\eta_{org}} \tag{17}$$

$$Sc_t = \frac{\eta_{org}}{D_{ZnA_2}} \tag{18}$$

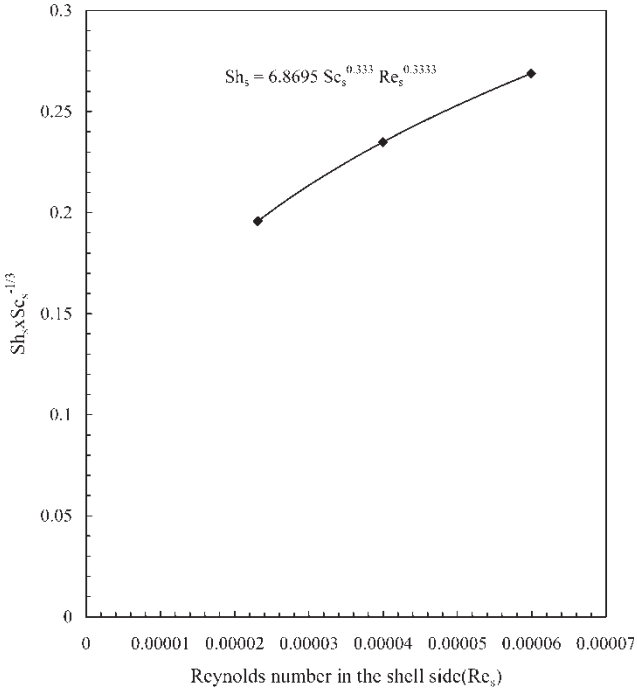

Figure 14. Mass transfer correlations in the shell side of Celgard Liqui-Cel extra-flow contactor.

Different parameters (n, L, d_i, d_a) are taken into account by the way of calculating the hydraulic diameter Eq. (10) and the mean velocity outside the fibers Eq. (11). The values of diffusion coefficients ($D_{Zn} = 6.42 \cdot 10^{-10}$ m/s and $D_{ZnA2} = 5.84 \cdot 10^{-10}$ m/s) necessary for calculation of Sh and Sc, are taken from Awakura et al.[37] for the tube side and Miyake et al.[38] for the shell side.

Corresponding to Figs. 13 and 14, the correlation that came out from the experimental results is:

$$\text{For the tube side: } Sh_t = 0.00281\, Re_t^{0.3334} Sc_t^{0.33} \left(\frac{d_i}{L}\right)^{0.333} \tag{19}$$

$$\text{For the shell side: } Sh_s = 6.8695\, Re_s^{0.3334} Sc_s^{0.33} \tag{20}$$

The linear plot of these figures shows the degree of reliability for the derived correlation. According to our knowledge, this is the first correlation describing the mass transfer of the aqueous flow in the tube side of cross flow HFM. For our tube side correlation, it was found to be very close to the Leveque approximation.

CONCLUSIONS

Microporous hollow fiber modules (HFMs) promise to be highly efficient devices for reactive solvent extraction. In this study, nondispersive solvent extraction was investigated for the removal of zinc ions from sulfuric acid solutions. Acidic organophosphorous extractant (D2EHPA) is investigated as a potential extracting agent. It seems that the extraction of zinc is highly pH dependent. Great dependence of the overall mass transfer coefficient on the concentration of a complexing agent is reported, where k_w increased from 5×10^{-6} m/s to 25×10^{-6} m/s for D2EHPA concentration ranged from 2v% to 8v%. The results clearly underline that the overall mass transfer coefficient depends on the aqueous and organic flow rates. Also, we observed that the zinc flux increased with increasing the aqueous flow rate. From the data obtained, we concluded that zinc extraction is controlled by the aqueous boundary layer resistance, the interfacial reaction resistance, and the organic boundary layer resistance in a hollow fiber membrane contactor.

NOMENCLATURE

A	membrane area at the interphase, m^2
C	solute concentration, M
d_i	internal membrane diameter, m
d_{lm}	log mean diameter, m
d_{hf}	outer membrane diameter, m
d_o	Hollow fiber diameter, m
D	Diffusivity, m^2/s
J	Flux, m mole/$m^2 \cdot s$
k	mass transfer coefficient, m/s
K	Equilibrium constant
L	length of hollow fiber, m
m	equilibrium distribution coefficient
n	number of hollow fiber in the module
Q	flow rate, m^3/s
Re	Reynolds number
Sc	Schmidt number
Sh	Sherwood number
V	Volume, m^3
v	Velocity, m/s

Greek Symbols

α	shell side correlation coefficient
β	shell side correlation coefficient

δ	membrane thickness, m
Δ	fractional resistance
τ	tortuosity
ε	porosity
η	kinematic viscosity, m^2/s

Subscripts

h	hydraulic
i	interfacial reaction
m	membrane
s	shell
so	outer shell
si	inner shell
t	tube
org	organic
w	aqueous
Zn	Zinc
ZnA_2	Zinc-D2EHPA complex

Superscripts

In	module inlet
out	module outlet
*	aqueous-organic interface

ACKNOWLEDGMENTS

We wish to thank the DAAD for a supporting grant and all the staff of Prof. H.-J. Bart for their helpful effort through this work.

REFERENCES

1. Logsdail, D.H.; Slater, M.J. *Solvent Extraction in the Process Industries*; Elsevier Applied Science: London, 1993.
2. Arnaud, B.; Juliane, F.; Herbert, E.S. Liquid-liquid extraction of aroma compounds with hollow fiber contactor. AIChE J. **2001**, *47*, 1780–1793.
3. Sekine, T. *Solvent Extraction 1990*; Elsevier: Amsterdam, 1992.
4. Marr, R.; Bart, H.-J.; Bouvier, A. Selective metal enrichment by liquid membrane permeation. Ger. Chem. Eng. **1981**, *4*, 209–216.
5. Ho, W.S.; Poddar, T.K. New membrane technology for removal and recovery of chromium from waste waters. Environ Progr. **2001**, *20*, 44–52.
6. Bart, H.-J.; Draxler, J.; Marr, R. Heavy metals recovery with extraction and permeation of incineration processes. Chem. Eng. Technol. **1990**, *13*, 313–318.
7. Sastre, A.M.; Kumar, A.; Shukla, J.P.; Singh, R.K. Improved techniques in liquid membrane separation: an overview. Sep. Purif. Methods **1998**, *27*, 213–298.

8. Kim, B.M. Membrane-based solvent extraction for selective removal and recovery of Metals. J. Membr. Sci. **1984**, *21*, 5–19.
9. Danesi, P.R. A simplified model for the coupled transport of metal ions through hollow-fiber supported liquid membranes. J. Membr. Sci. **1984**, *20*, 231–248.
10. Kiani, A.; Bhave, R.R.; Sirkar, K.K. Solvent extraction with immobilized interfaces in a microporous hydrophobic membrane. J. Membr. Sci. **1984**, *20*, 125–145.
11. Dahuron, L.; Cussler, E.L. Protein extraction with hollow fibers. AIChE J. **1988**, *34*, 130–136.
12. Li, K.; Tan, X.Y. Mass transfer and chemical reaction in hollow-fiber membrane reactors. AIChE J. **2001**, *47* (2), 427–435.
13. Campderros, M.E.; Acosta, A.; Marchese, J. Selective separation of copper with Lix864 in a hollow fiber module. Talanta **1998**, *47*, 19–24.
14. Tatjana, M.T.; Goran, T.V.; Jozef, J.C. Dispersion-free solvent extraction of thallium (IV) in hollow fiber contactors. Sep. Sci. Tech. **2000**, *35* (10), 1587–1601.
15. Kubota, F.; Goto, M.; Nakashio, F. Extraction kinetics of rare earth metals with 2-ethylhexyl phosphonic acid mono-2-ethylhexyl ester using a hollow fiber membrane extractor. Sep. Sci. Tech. **1995**, *30* (5), 777–792.
16. Daiminger, U.; Nitsch, W.; Plucinski, P.; Geist, A. Nondispersive chemical extraction in hollow fiber modules, Proceedings of ISEC'96- Value Adding Through Solvent Extraction, March 19–23, 1996, Shallcross, D.C., Paimin, R., and Prvcic, L.M., Eds.; Melbourne, Australia, 1996, 1161–1166.
17. Yoshizuka, K.; Yasukawa, R.; Koba, M.; Inoue, K. Diffusion model accompanied with aqueous homogeneous reaction in hollow fiber membrane extractor. J. Chem. Eng. Japan **1995**, *28* (1), 59–65.
18. Prasad, R.; Sirkar, K.K. Dispersion-free solvent extraction with microporous hollow fiber membrane. AIChE J. **1988**, *34* (2), 177–188.
19. Costello, M.J.; Fane, G.A.; Hogan, P.A.; Schofield, R.W. The effect of shell side hydrodynamics on the performance of axial flow hollow fiber modules. J. Membr. Sci. **1993**, *80*, 1–11.
20. Chang, H.Y.; Prasad, R.; Guha, A.K.; Sirkar, K.K. Hollow fiber solvent extraction removal of toxic heavy metals from aqueous waste streams. Ind. Eng. Chem. Res. **1993**, *32*, 1186–1195.
21. Ilias, S.; Schimmel, K.A.; Yezek, P.M. Nondispersive liquid-liquid extraction of copper and zinc from an aqueous solution by DEHPA and LIX984 in a hollow fiber membrane module. Sep. Sci. Tech. **1999**, *34*, 1007–1019.
22. Valenzuela, F.; Aravena, H. Separation of Cu(II) and Mo(VI) from mine waters using two microporous membrane extraction systems. Sep. Sci. Tech. **2000**, *35* (9), 1409–1421.
23. Alexander, P.R.; Callahan, R.W. Liquid-liquid extraction and stripping of gold with macroporous hollow fibers. J. Membr. Sci. **1987**, *35*, 57–71.
24. He, D.; Luo, X..; Yang, C.; Ma, M.; Wan, Y. Study of transport and separation of Zn(II) by a combined supported liquid membrane/strip dispersion process containing D2EHPA in kerosene as the carrier. Desalination **2006**, *194*, 40–51.
25. Ortiz, I.; Bringas, E.; San Román, M.F.; Urtiaga, A.M. Selective Separation of Zinc and Iron from Spent Pickling Solutions by Membrane- Based Solvent Extraction: Process Viability. Sep. Sci. Tech. **2004**, *39* (10), 2441–2455.
26. Juang, R.-S.; Kao, H.-C. Extraction separation of Co(II)/Ni(II) from concentrated HCl solutions in rotating disc and hollow-fiber membrane contactors. Sep. Purif. Tech. **2005**, *42*, 65–73.
27. Yang, C.; Cussler, E.L. Reaction dependent extraction of copper and nickel using hollow fibers. J. Membr. Sci. **2000**, *166*, 229–238.

28. Bart, H.-J.; Stevens, G.W. Reactive solvent extraction. In *Ion Exchange and Solvent Extraction*; Marcus, Y. and Sengupta, A.K. Eds.; Marcel Dekker: New York, 2004, Vol. 17, 37–82.
29. Prasad, R.; Sirkar, K.K. Membrane based solvent extraction. In *Membrane Handbook*; Van Nostrand Reinhold: New York, 1992, pp. 727–763.
30. Ho, W.S.W.; Sirkar, K.K. *Membrane Handbook*; Van Nostrand Reinhold: New York, 1992.
31. Crowder, R.O.; Cussler, E.L. Mass transfer resistances in hollow fiber pervaporation. J. Membr. Sci. **1997**, *134*, 235–244.
32. Wang, E.L.; Cussler, E.L. Baffled membrane modules made with hollow fiber fabric. J. Membr. Sci. **1993**, *85*, 265–278.
33. Schoner, P.; Plucinski, P.; Nitsch, W.; Daiminger, U. Mass transfer in the shell side of cross flow hollow fiber modules. Chem. Eng. Sci. **1998**, *53*, 2319.
34. Daiminger, U.; Geist, A.G.; Nitsch, W.; Plucinski, P. Efficiency of hollow fiber modules for non-dispersive chemical extraction. Ind. Eng. Chem. Res. **1996**, *35*, 184–191.
35. Yang, Z.F.; Guha, A.K.; Sirkar, K.K. Novel membrane-based synergistic metal extraction and recovery processes. Ind. Eng. Chem. Res. **1996**, *35*, 1383–1394.
36. Kosaraju, P.B.; Sirkar, K.K. Novel solvent-resistant hydrophilic hollow fiber membranes for efficient membrane solvent back extraction. J. Mem. Sci. **2007**, *288*, 41–50.
37. Awakura, Y.; Doi, T.; Majima, H. Dteremination of the diffusion coefficients of $CuSO_4$, $ZnSO_4$, and $NiSO_4$ in aqueous solution. Metall. Trans. B. **1988**, *19B*, 5–12.
38. Miyake, Y.; Matsuyama, H.; Nishida, M.; Nakai, M.; Nagase, N.; Teramoto, M. Kinetics and mechanism of metal extraction with acidic organophosphorous extractants (I): Extraction rate limited by diffusion process. Hydrometallurgy **1990**, *23*, 19–35.